Geomechanics and Engineering, *Vol. 30, No. 4 (2022) 373-382*
https://doi.org/10.12989/gae.2022.30.4.373

Soil water retention and hysteresis behaviors of different clayey soils at high suctions

Ze Li[1], You Gao*[1], Haihao Yu[2], Bo Chen[3] and Long Wang[4]

[1]*School of Civil and Environmental Engineering, Ningbo University, 818 Fenghua Road, Ningbo 315211, China*
[2]*Laboratory of Geomechnics and Geotechnical Engineering, Guilin University of Technology, 12 Jian Gan Road, Guilin, 541004, China*
[3]*College of Civil Engineering and Architecture, Quzhou University, 78 Jiuhua Road, Quzhou 324000, China*
[4]*School of Environment and Civil Engineering, Jiangnan University, Wuxi, 214122 ,China*

(*Received November 29, 2021, Revised April 23, 2022, Accepted July 24, 2022*)

Abstract. Unsaturated soil at high suctions is widespread. Many civil engineering projects are related to the hydro-mechanical behavior of unsaturated soils at high suctions, particularly in arid and semiarid areas. To investigate water retention behaviors of nine clayey soils (one is classified as fat clay and the others are classified as lean clay according to the unified soil classification system), the high suction (3.29-286.7 MPa) was imposed on the specimens at zero net stress by the vapor equilibrium technique. In this paper, the effect of void ratio on the water retention behavior at high suction was discussed in detail. Validation data showed that soil types, i.e., different mineralogical compositions, are critical in the soil water retention behavior at a high suction range. Second, the hysteresis behavior at a high suction range is mainly related to the clay content and the specific surface area. And the mechanism of water retention and hysteresis behavior at high suctions was discussed. Moreover, the maximum suction is not a unique value, and it is crucial to determine the maximum suction value accurately, especially for the shear strength prediction at high suctions. If the soil consists of hydrophilic minerals such as montmorillonite and illite, the maximum suction will be lower than 10^6 kPa. Finally, using the area of hysteresis to quantify the degree of hysteresis at a high suction range is proposed. There was a good correlation between the area of hydraulic hysteresis and the specific surface area.

Keywords: high suction; hysteresis behavior; soil water retention behavior; unsaturated soil

1. Introduction

The soil water characteristic curve (SWCC), also called the soil water retention curve, represents a soil's ability to store and release water (Fredlund and Rahardjo 1993). In recent decades, many tests have been conducted to investigate the soil water retention behavior of unsaturated soils at low suctions (0-1500 kPa) based on the axis-translation technique (Miller *et al*. 2002, Yang *et al*. 2004, Zhou *et al*. 2014, Al-Mahbashi *et al*. 2015, Wu *et al*. 2020). However, the test results regarding the soil water retention behavior (such as hysteresis behaviors, maximum suction value, residual point determined, etc.) of different unsaturated soils at high suctions are still very limited in the literature, especially for the clayey soils. Therefore, the soil water retention behaviors at high suctions require a comprehensive analysis, which can lead to a better understanding of the SWCC of clayey soils in the full suction range.

The soil water retention behavior is closely related to the water flow, consolidation, deformation processes, and shear strength of unsaturated soils (Vanapalli *et al*. 1999, Konrad and Lebeau 2015, Gao *et al*. 2018, Sun and Cui 2020, Niu *et al*. 2020, Rasool and Kuwano 2020, Wang *et al*. 2020, Gao *et al*. 2021, Chen *et al*. 2022, Tan *et al*. 2022, Wang *et al*. 2022). The SWCC can be indirectly related to predicting shear strength, tensile strength, and permeability. That is, the parameter chi (χ) of many shear strength equations was related to the effective degree of saturation or volumetric water content, i.e., the soil suction was determined by the SWCC. In general, the parameter χ is equal to the effective degree of saturation (S_e=S_r-S_{re}/100-S_{re}). S_r and S_{re} is the degree saturation and the residual degree saturation, determined by the geometrical relationship based on the soil water retention test results at high suctions.

In many cases, the maximum suction (s_m) of the SWCC was regarded as constant (i.e., 10^6 kPa), but the maximum suction was not a unique value. This will affect the fitting results of the soil water characteristic curve. Suppose the soil water characteristic curve cannot be accurately fitted. In that case, there is a significant error in the unsaturated contribution term (i.e., the term of $\chi\tan\varphi''$, φ'' is the effective friction) for unsaturated shear strength prediction. Therefore, the soil water retention behavior at high suctions is essential for many applications in geotechnical engineering.

This paper presents a systematic study to investigate the soil water retention behaviors of different soils. SWCCs of different clayey soils at high suctions (3.29-286.7 MPa) are measured by the vapor equilibrium technique. A comprehensive analysis of the mechanism of water retention and hysteresis behavior at high suctions were discussed. By analyzing the experimental data, the influences of adsorption capacity on SWCCs of different

*Corresponding author, Associate Professor
E-mail: gaoyou@nbu.edu.cn

ISSN: 2005-307X (Print), 2092-6219 (Online)

Table 1 Physicochemical index properties of the nine soils

Nos.	Initial water content (%)	Density (kg/m^3)	Specific gravity	Initial void ratio	LL (%)	PI (%)	Clay content (%)	SSA (m^2/g)	USCS
S1	39.5	1.84	2.73	1.08	53.75	28.01	50.5	93.79	CH
S2	47.7	1.75	2.73	1.30	49.07	22.69	47.1	107.65	CL
S3	29.5	1.89	2.72	0.86	32.72	14.51	23.4	42.8	CL
S4	30.4	1.89	2.72	0.87	43.99	19.4	28.4	61.7	CL
S5	33.3	1.84	2.72	0.97	32.07	11.33	22.5	34.25	CL
S6	34.2	1.87	2.72	0.95	48.85	29.17	34.4	69.32	CL
S7	33.9	1.85	2.70	0.95	32.41	12.66	20.7	28.54	CL
S8	21.5	1.95	2.70	0.68	41.62	20.59	42.7	46.49	CL
S9	33.4	1.81	2.68	0.94	39.59	14.87	5.62	16.31	CL

Note: LL = liquid limit; PI = Plastic index; SSA=Specific surface area; USCS=Unified soil classification system

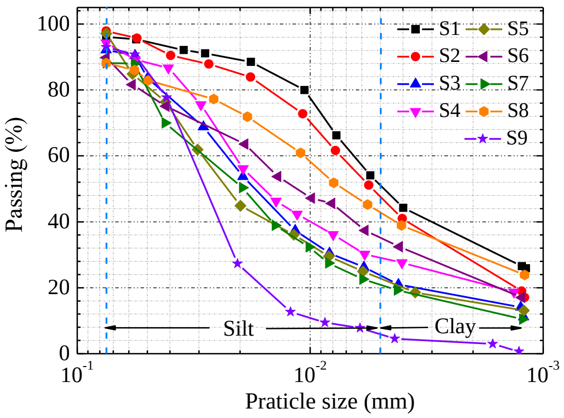

Fig. 1 The grading curve

(a) Sample preparation (b) Sealed container

Fig. 2 Test processes of the VET

soils at high suctions are obtained based on the microstructure and specific surface area test results. Finally, using the area of hysteresis to quantify the degree of hysteresis at a high suction range is proposed.

2. Experimental techniques and testing program

2.1 Experimental techniques

A total of nine natural clayey soils were used. Some physicochemical index properties of the soils, such as specific gravity, plastic index, liquid limit, initial water content, and specific surface area are summarized in Table 1. Specific surface area of the nine soils was measured by nitrogen adsorption method. The undisturbed samples with a diameter of 10 cm and a height of 30 cm were directly taken from in situ to laboratory by thin wall sampling method. Then the specimens were prepared in a stainless steel specimen ring with 6.18 cm inside diameter and 2 cm height. The grading curves of different soils are shown in Fig. 1. The SWCCs in the high total suction range (3.92-286.7 MPa) for drying and wetting were measured using a vapor equilibrium technique (VET).

2.2 Testing procedure

The VET is commonly employed to control high suctions. The VET usually uses a saturated salt solution to generate constant total suction conditions in a sealed container. Greenspan (1977) collected the relative humidity of saturated salt solutions, as shown in Table 2. The total suctions can be calculated using Kelvin's law (Fredlund and Rahardjo 1999), as follows

$$\psi = -\frac{\rho_w RT}{w_v}\ln(RH) \quad (1)$$

where, ψ is the total suction, kPa. w_v is the molecular mass of water vapor, which is assumed to be equal to 18.016 g/mol, and R is the universal gas constant (i.e., 8.31432 J/mol K). ρ_w is the density of water, T is the absolute temperature, and RH is the relative humidity, %.

Seven sealed containers with seven supersaturated salt solutions (see Table 2) were used to obtain different suctions after vapor equilibrium (see Fig. 2(b)). To reduce the equilibrium time, the samples for the drying and wetting tests were prepared by cutting the specimen above into six pieces using the wire saw (see Fig. 2(a)). Two irregular small piece samples were needed in each sealed container for drying or wetting test. One piece is used to measure the water content and another is used to measure the volume of irregular samples based on Archimedes' principle. For the drying test, irregular samples were put on the upper partition of each sealed container at zero net stress, while supersaturated solutions were stored in the lower partition (see Fig. 2(b)). For the wetting test, the samples were oven dried first and then were placed on the upper partition of containers with seven supersaturated salt solutions. The samples need approximately two months to reach equilibrium, and the equilibrium state was checked by weighing the samples until the weekly difference was less than 0.1 g (Cai *et al*. 2020).

The volume measurement procedure for the irregular soil

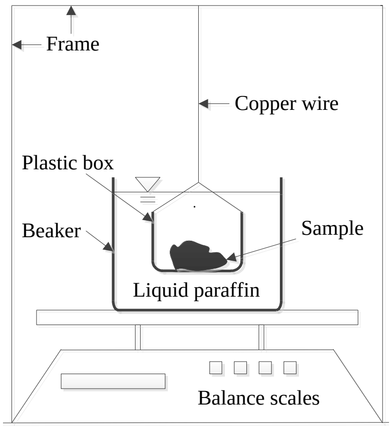

Fig. 3 Sketch of volume measurement (modified from Sun *et al*. 2016)

Table 2 Saturated salt solution and corresponding suction (20°C)

Saturated salt solutions	RH (%)	Total suction (MPa)
LiCl	12.0	286.70
$MgCl_2$	33.1	149.51
NaBr	59.1	71.12
NaCl	75.5	38.00
KCl	85.1	21.82
KNO_3	94.6	7.48
K_2SO_4	97.6	3.29

sample can be referenced in Sun *et al*. (2016) as follows: (1) the soil pieces were immersed into liquid paraffin for about 15 minutes for filling with the soil surface pores, (2) the soil was taken out from the liquid paraffin and the excess liquid paraffin was wiped on the soil surface, (3) the balance values were recorded before and after the soil immersed into the liquid paraffin (see Fig. 3). Then the volume of the soil pieces can be determined by the buoyant force divided by the density of the liquid paraffin.

3. Results and discussion

3.1 Effect of void ratio on SWCC at high suctions

For the same soil type, the effect of stress states on the SWCC can be attributed to the void ratio change at low suctions (<1500 kPa). Sun *et al*. (2007) reported that the SWCC depends mainly on the current density or void ratio and not directly on the stress state at low suctions. In recent years, many researchers have reported the effect of void ratio on the soil water retention behavior at high suctions (>1500 kPa), and pointed out that the SWCCs in terms of the relation between the gravimetric water content and suction are independent of the initial void ratios at high suctions (Romero *et al*. 1999, Birle *et al*. 2008, Salager *et al*. 2013, Gao and Sun. 2017, Cai *et al*. 2020). In the high suction range, the critical factors of the SWCC are soil types (i.e., mineralogical composition), not dry density.

Fig. 4 shows the SWCCs of different soils (data from

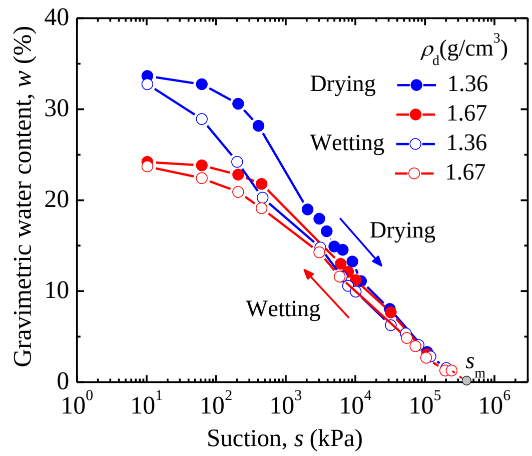

(a) SWCCs of Boom clay (data from Romero *et al*. 1999)

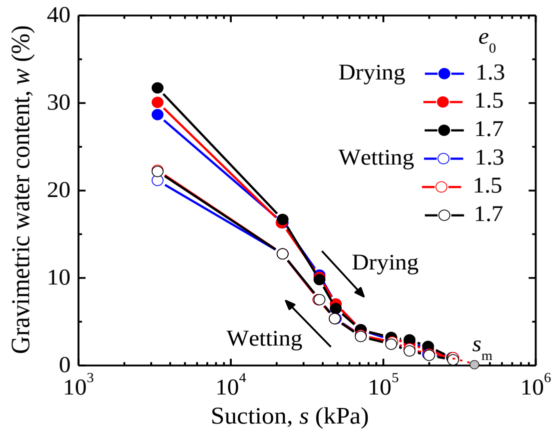

(b) SWCCs of Lateritic soil (data from Cai *et al*. 2020)

Fig. 4 SWCCs of different soils over a wide suction and at high suctions

Romero *et al*. 1999, Cai *et al*. 2020) with various initial dry densities or void ratios over a wide suction and at high suctions. In the figures, the drying and wetting SWCCs are independent of the dry density or void ratio at high suctions. In the high suction range, the effect of the initial dry density or void ratio on the SWCCs is barely noticeable. Soil type (i.e., different mineralogical compositions) is critical for the soil water retention behavior at a high suction range. Therefore, it is worthwhile to investigate the effect of different soils on the soil water retention behavior at a high suction range.

3.2 Effect of soil types on hysteresis behavior at high suctions

Fig. 5 shows the test results of the SWCCs under both drying and wetting conditions for nine soils at high suctions. From the figures, the gravimetric water content of specimens S1, S2, S4, and S6 is greater than that of specimens S3, S5, S7, S8, and S9 under the same suction. The water retention behavior of specimens S1, S2, S4, and S6 is better than that of specimens S3, S5, S7, S8 and S9 at high suctions. A typical SWCC cannot explain the mechanism of water retention behavior due to capillary action at low suctions (<1500 kPa). At a low suction range,

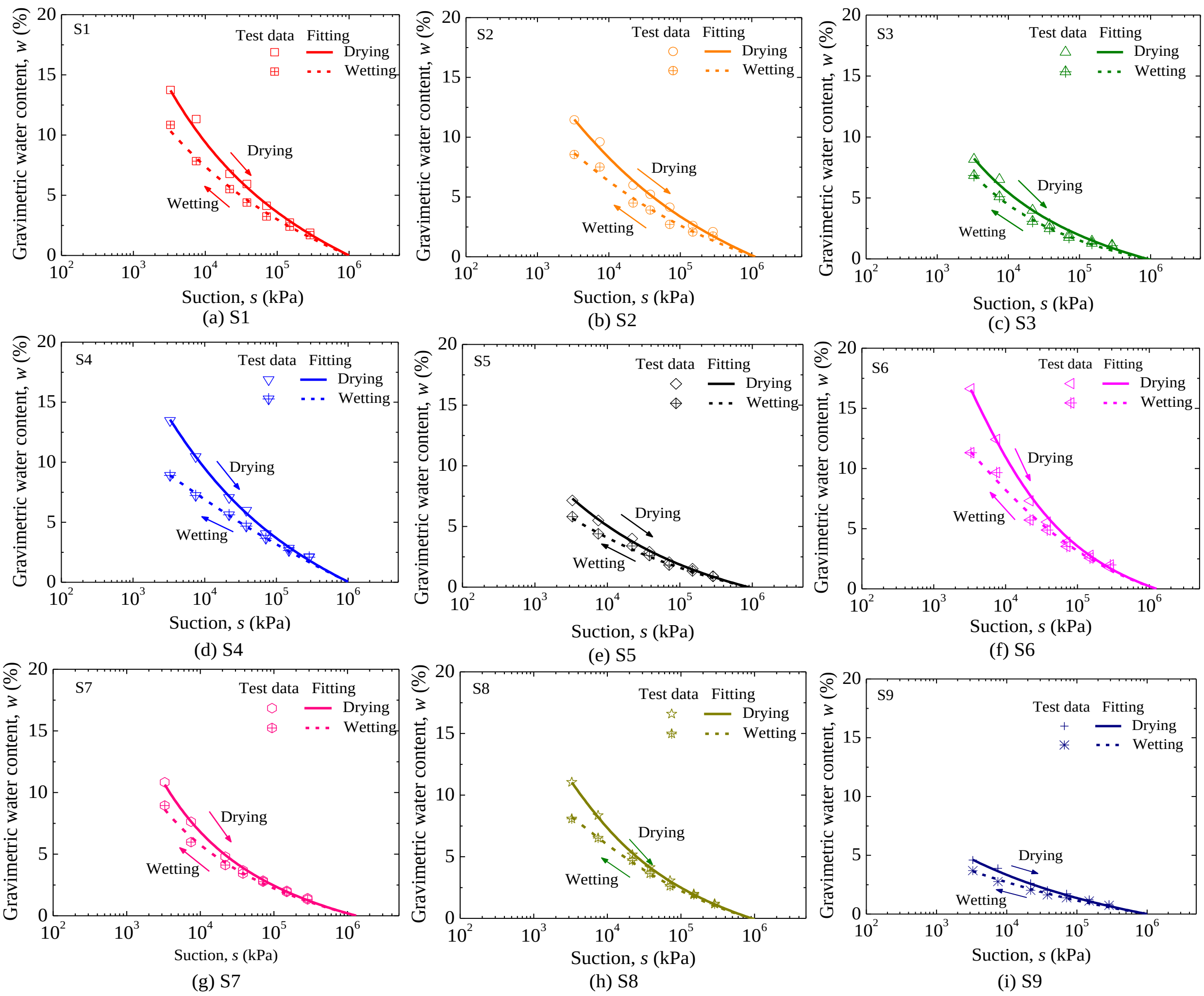

Fig. 5 Drying and wetting SWCCs of the nine soils

the higher the clay content is, the better the water retention capacity is. For the same soil, a smaller void ratio presented a better water retention capacity. However, the water retention capacity of specimen S8 (with a fine gradation curve and a small initial void ratio, see Fig. 1 and Table 1) is worse than that of specimens S4 or S6 at the high suction range shown in Fig. 5. In addition, all the SWCCs present hysteresis behavior at high suctions. The hydraulic hysteresis of specimens S1, S2, S4, and S6 is more apparent than the hysteresis of specimens S3, S5, S7, S8, and S9. At a high suction range, hysteresis behavior cannot be explained by the conventional conceptual mechanisms for hydraulic hysteresis at low suctions, such as the ink-bottle pore neck and solid-liquid-contact angle. The water retention behavior depends on the adsorption capacity of the soil particle.

The X-ray diffraction (XRD) analysis results for the nine test soils are shown in Fig. 6. Some minerals such as quartz and albite are observed in all soils, while montmorillonite is found only in specimens S1, S2, and S4. For a soil consisting of high content of hydrophilic minerals such as montmorillonite and illite, there exists significant hydraulic hysteresis in specimens S1, S2, S4. The water retention behavior of specimens S1, S2, S4 is also better than that of specimens S3, S5, S7, S8 and S9 at high suctions (see Fig. 5). Moreover, the specimens S1, S2, and S4 have high liquid limit and larger specific surface area (see Table 1) due to its consisting of hydrophilic minerals. But only barely noticeable hysteresis exists in specimens S3, S5, S7, S8 and S9 is mainly attributed to its high content of none hydrophilic minerals (such as quartz, chlorite, muscovite and albite) and low content of hydrophilic minerals.

Fig. 7 shows scanning electron microscope (SEM) micrographs of the nine soils with a magnification of 2000. In Fig. 7 (d), (g), and (i), pores with a wide variety of sizes can be observed (note that the dark zones are the pore space). Large pores are generally formed between aggregates, while smaller ones exist within aggregates, as shown in Fig. 7(g) and Fig. 7(i). That is, the ink-bottle pore neck exists in specimens S7 and S9. According to conventional conceptual mechanisms for the hydraulic hysteresis at low suctions, specimens S7, and S9 may present apparent hydraulic hysteresis phenomenon. However, specimens S7, and S9 present barely noticeable hydraulic hysteresis behavior at high suctions. The hysteresis behavior in high suction range is mainly related to water film adsorption, the clay content, and the specific

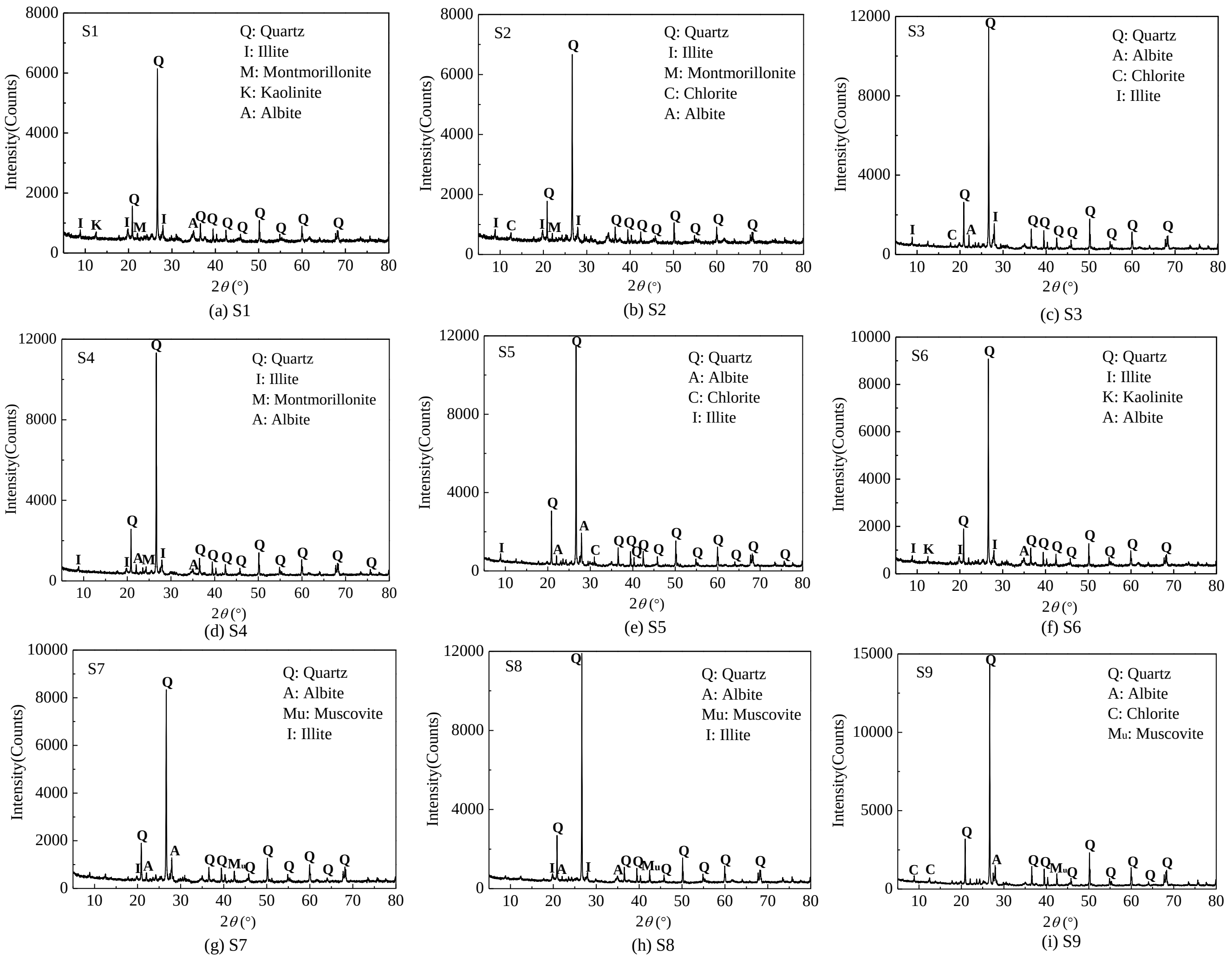

Fig. 6 X-ray diffraction test results of the nine soils

surface area. In Fig. 7 (a), (b), (d), and (f), the SEM micrographs of samples S1, S2, S4, and S6 present dense lamellar microstructures, and samples S1, S2, S4, and S6 show apparent hysteresis behavior (See Fig. 5). The sample with a dense lamellar microstructure also has an appropriately large specific surface area due to it consisting of hydrophilic minerals such as montmorillonite and illite (see Fig. 6), such as specimens S1, S2, S4, and S6 (see Table 1). Therefore, hysteresis behavior at high suctions is mainly related to the microstructure, hydrophilic minerals content, clay content, or specific surface area. The relationships between the hysteresis behavior and physical indices are discussed in the below section.

Fig. 8 shows the drying and wetting SWCCs of different soils, which were extracted from Fig. 5. The figures show that the drying and wetting SWCCs of specimen S6 are the highest at suction ranges from 3.29 to 50 MPa. When the suction is higher than approximately 50 MPa, the drying curves of specimens S1, S2, S4, and S6 are almost the same. The clay content and the specific surface area of S6 are smaller than those of S1 and S2. However, the microstructure of S6 exhibits a very dense micropore structure, as shown in Fig. 7. That is, the microstructure is a critical factor that affects the water retention behaviors at high suctions.

Moreover, it is worth noticing that the drying and wetting SWCCs of specimens S7 and S8 are almost the same. The clay content and the specific surface area of S7 are twice those of S8; there were much larger significant differences in the microstructure of specimen S7 (regular lamellar structure) and specimen S8 in Fig. 7. This means that the clay content and specific surface area can affect the water retention behaviors; the microstructure also has a significant influence. The drying and wetting SWCCs of specimens S3 and S5 are close, and the water retention behavior of the S3 and S5 is worse than that of specimens S1, S2, S4, and S6. The pores with a wide variety of sizes can be observed in specimens S3 and S5, while the photos of specimens S1, S2, S4, and S6 exhibit dense microstructures. In addition, the specimens S9 present worse water retention behaviors, due to their microstructure with the large aggregates (see Fig. 7 i) and small specific surface area (in Table 1).

3.3 Effect of the maximum suction on shear strength prediction

The maximum suction is not a unique value in Fig. 8.

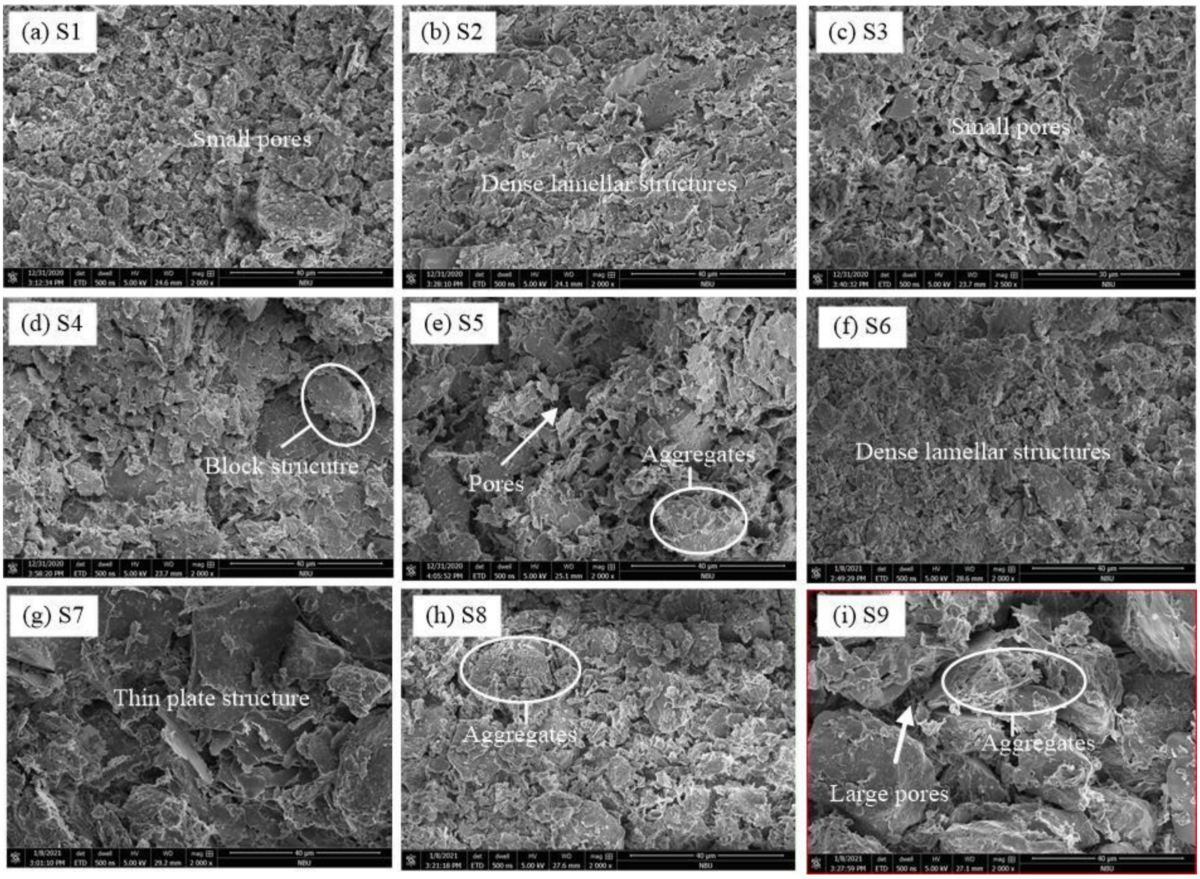

Fig. 7 SEM micrographs of the nine soils

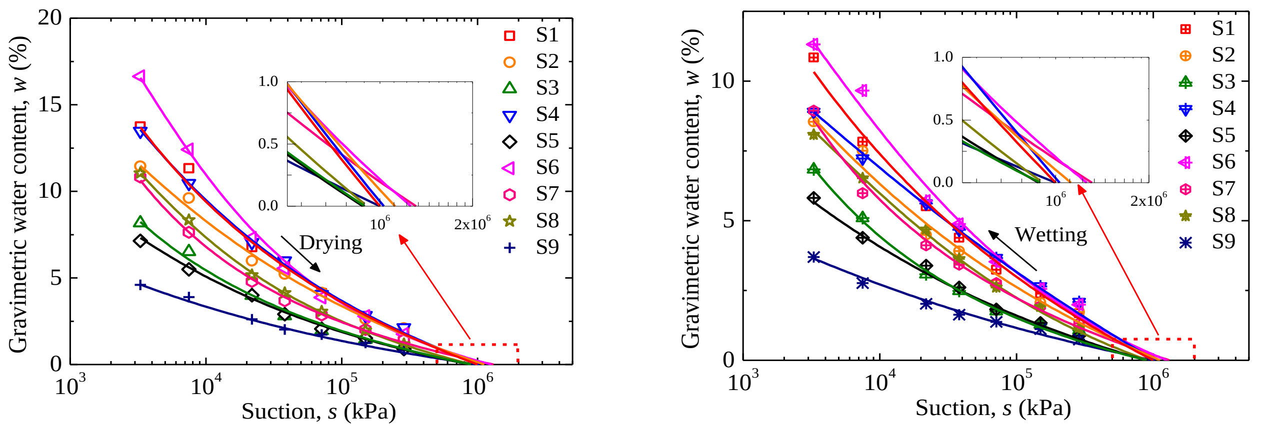

(a) Drying curves

(b) Wetting curves

Fig. 8 SWCCs of the nine soils during the drying

The maximum suction varies from 880 to 1310 MPa. Similar results have been found in literatures. For example, Lu *et al*. (2015) found that the maximum suction varies from 475 to 1180 MPa, and depends on soil mineralogy. Mineral composition controls the physicochemical forces between soil solids and water through the specific surface area (Zhou and Lu 2021).

Fig. 9 shows the experimental dataset of a broad suite of 10 soils with hydrophilic minerals (such as montmorillonite, and illite) from the literature. The soil composition and mineralogy of the ten soils were collected Table 3. At a high suction range, the SWCCs in terms of water content decrease sharply as the suction increases. All the SWCCs present an almost linear relation between the water content and the logarithmic coordinates of suction. The residual points of the SWCCs of expansive soil, and bentonite are hard to determine by the graphical method. In addition, it is worth noticing that the maximum suctions of different soils with hydrophilic minerals are smaller than 10^6 kPa. The maximum suction approximately varies from 420 to 650 MPa.

It is crucial to determine the maximum suction value accurately. In general, the unsaturated effective stress parameter χ is equal to the degree of saturation or the

Table 3 Geotechnical properties, soil composition, and mineralogy of the 10 soils

Soil no.	Reference	Soil name	Specific gravity	Plastic index	Void ratio	Mineral composition
1	Ito and Azam (2013)	Vertisolic expansive soil	2.75	52.7	0.6	The main mineral component is smectite, illite, and chlorite, etc.
2	Zhang *et al.* (2019)	Nangyang expansive soil	2.74	21.6	0.83, 1.03, and 1.19	62% quartz, 9.9% illite and 5.8% montmorillonite, etc.
3	Zhu *et al.* (2016)	Ca-GMZ bentonite	2.73	58	1.02	The dominant mineral is montmorillonite.
4	Ajdari *et al.* (2013)	silt–bentonite mixture	2.67	32	0.78	60% quartz, 20% montmorillonite, 11% feldspar, etc.
5	Romero *et al.* (1999)	Boom clay	2.69	27	0.58, 0.92	20–30% kaolinite,20–30% illite, 10–20% smectite, etc.
6	Teipathy *et al.* (2014)	MX80 bentonite	2.8	374	No data	The dominant mineral is montmorillonite.
7	Baille *et al.* (2014)	Calcigel bentonite	2.8	121.9	No data	The dominant mineral is montmorillonite.
8	Baille *et al.* (2014)	NX illite	2.71	45.5	No data	The dominant mineral is illite.
9	Péron *et al.* (2007)	Bioley clayey silt	2.71	14.9	0.83	The soil contains quartz, calcite , illite, smectite, etc.
10	Zhou *et al.* (2021)	Ningming expansive soil	2.73	127	0.52	The soil contains quartz, illite, smectite, etc.

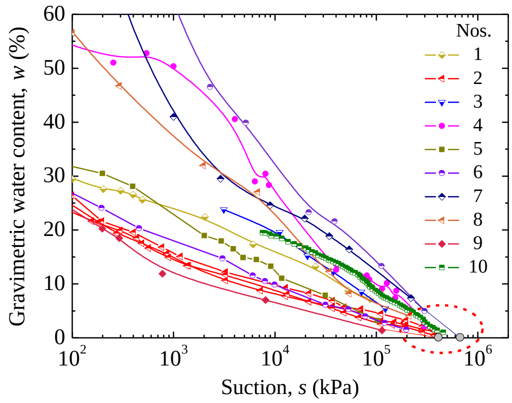

Fig. 9 SWCCs data (suction versus gravimetric water content) for the 10 Soils

effective degree of saturation. Suppose the soil water characteristic curve cannot be accurately fitted at high suctions due to using the incorrect maximum suction value. In that case, there is a significant error in the unsaturated contribution term for unsaturated shear strength prediction at a high suction range. The unsaturated contribution term τ_{us} can be expressed as follow

$$\tau_{us} = s\chi \tan\phi' = sS_r \tan\phi' \tag{2}$$

where, s is the suction, S_r is the degree of saturation, ϕ' is the effective internal friction angle.

Fig. 10 shows the values of sS_r in Eq. (2) calculated using the fitting curves (Fitted using Fredlund and Xing's 1994 equation). The SWCCs data in terms of the degree of saturation was from the reference by Romero *et al.* (1999). It can be seen if the maximum suction (s_m) was set a unique value (s_m=1000 MPa), the values of sS_r (see Fig. 10(b)) is obviously overestimate at a high suction range. This will lead to obviously overestimate the shear strength of unsaturated soils at a high suction range, especially for clayey soils including the hydrophilic minerals. Therefore, the maximum suction is not a unique value, and it is crucial to determine the maximum suction value accurately, especially for the shear strength prediction at high suctions.

3.4 Quantifying hydraulic hysteresis

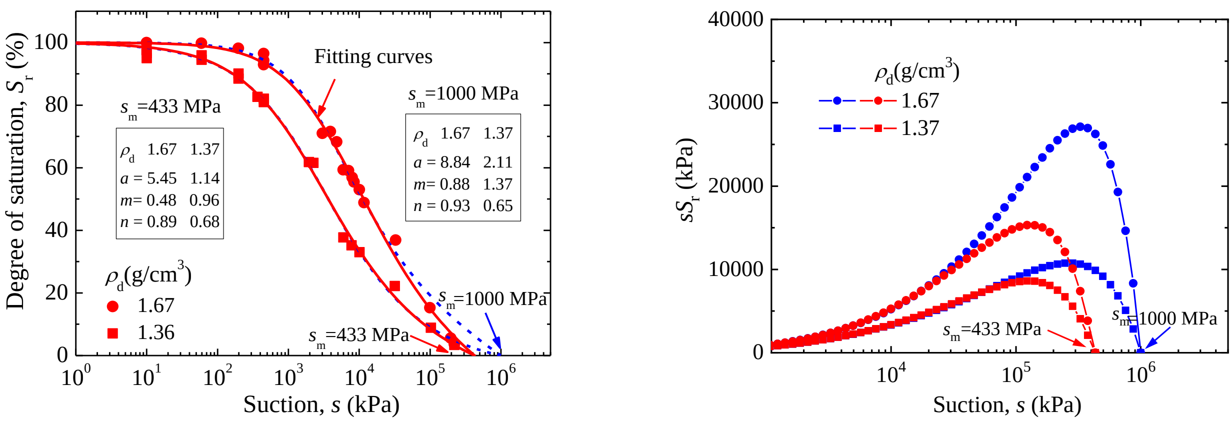

(a) Fitting curves (data from Romero *et al.* 1999) (b) Curves of the sS_r values

Fig. 10 Values of sS_r calculated using the fitting curves

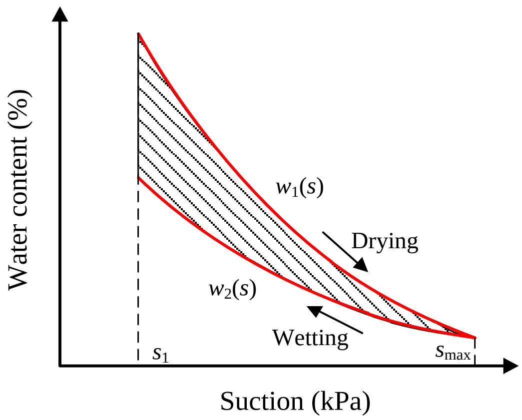

Fig. 11 Definition of the area of hydraulic hysteresis

To quantify the degree of hysteresis at a high suction range, the area of hysteresis is proposed here. As illustrated in Fig. 11, the area of hysteresis (AH) evaluates the hysteresis in the suction space and is defined as

$$AH=\int_{s_1}^{s_2}[w_1(s)-w_2(s)]ds \tag{3}$$

where, s is suction, kPa; $w(s)$ is the SWCC fitting function. Fredlund and Xing's (1994) equation is also a popular fitting function. In terms of the relations between the water content and logarithmic suction, the equation with a correction factor C(s) is given by

$$\begin{aligned} w(s) &= C(\mathrm{s})\frac{w_s}{\{\ln[e+(s/a)^n]\}^m} \\ &= (1-\frac{\ln(1+s/s_{re})}{\ln[1+(s_m/s_{re})]})\frac{w_s}{\{\ln[e+(s/a)^n]\}^m} \end{aligned} \tag{4}$$

where, w_s is the saturated water content, e is the natural number (equal to 2.71828), a, n and m are the fitting parameters, and s_{re} is the residual suction value. s_m is the maximum suction corresponding to the dry state. Lu and Khorshidi (2015) pointed out that the maximum suction varies from 475 to 1180 MPa. Therefore, s_m can be regarded as fitting parameter. In addition, when s_{re} ranges from 1.5 to 3 MPa (Fredlund and Xing 1994), satisfactory approximation fitting results can be obtained using Eq. (4). For simplicity, s_{re} is assumed to be 1.5 MPa in Eq. (4). Calculated parameters for various soils (in Fig. 5) based on Fredlund and Xing's equation in Table 3. The area of hysteresis (AH) can be calculated by the approximation numerical integration method.

Fig. 12(a) shows the relationship between the area of hydraulic hysteresis and the specific surface area. There was a good correlation between the area of hydraulic hysteresis and the specific surface area with a coefficient of determination greater than or equal to 0.901. The relationship between the area of hydraulic hysteresis (AH) and the specific surface area (SSA) can be expressed as

$$AH=ae^{\frac{SSA}{b}} \tag{5}$$

where a and b are fitting parameters, and the recommended values of a and b are 743 and 76 in Eq. (5) for nine soils in this paper, respectively. The total adsorptive water content is related to the total SSA. The SSA includes a soil particle surface and interlamellar crystalline surface. Adsorptive water on the interlamellar crystalline surface is mostly occurs through interaction between exchangeable cations and water molecules (Zhou and Lu 2021). The volume of the interlamellar crystalline surface affects the adsorptive water content during wetting and drying. However, the correlation between the area of hydraulic hysteresis and the clay content was examined, as illustrated in Fig. 12(b). There was a week correlation between the area of hydraulic hysteresis and the clay content. Different soils always have mineral compositions. The clay content is related to the total specific surface area, but it does not really reflect the adsorptive water content.

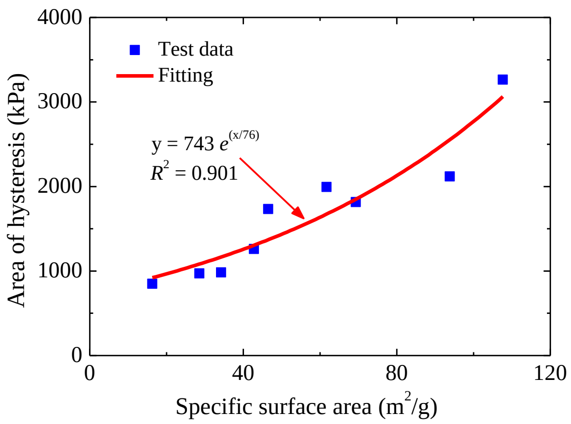

(a) Specific surface area

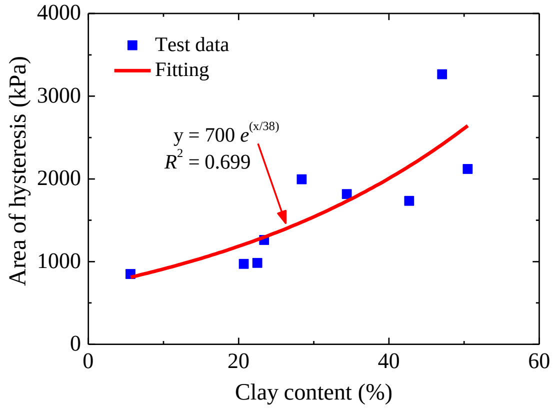

(b) Clay content

Fig. 12 Area of hydraulic hysteresis versus specific surface area and clay content

4. Conclusions

In this paper, a comprehensive analysis of drying and wetting SWCCs of nine clayey soils was performed at high suctions. The main conclusions are obtained as follow:

(1) The mechanism of water retention and hydraulic hysteresis behavior at high suctions is cannot be explained by typical SWCC at low suctions, such as ink-bottle pore neck and solid-liquid-contact angle. The

water retention behavior is closely related to the specific surface area, hydrophilic minerals content and microstructure at high suctions. Moreover, it is crucial to determine the maximum suction value accurately, especially for the shear strength prediction at high suctions.

(2) The maximum suction is not a unique value. The maximum suction will be smaller than 10^6 kPa if the soil contains hydrophilic minerals such as montmorillonite and illite. In addition, the residual points are hard to determine by the graphical method.

(3) Using the area of hysteresis to quantify the degree of hysteresis at a high suction range is proposed. There was a good correlation between the area of hydraulic hysteresis and the specific surface area. The total adsorptive water content is related to the total specific surface area.

Acknowledgment

The authors express their gratitude for the grants provided by the National Natural Science Foundation of China (No. 41902279), Guangxi Key Laboratory of Geomechanics and Geotechnical Engineering (No. 20YKF06), the Fundamental Research Funds for the Provincial Universities of Zhejiang (No. SJLY2022007), and the Natural Science Foundation of Jiangsu Province (No. BK20210479).

References

Ajdari, M., Habibagahi, G. and Masrouri, F. (2013), "The role of suction and degree of saturation on the hydro-mechanical response of a dual porosity silt-bentonite mixture", *Appl. Clay Sci.*, **83**, 83-90. https://doi.org/10.1016/j.clay.2013.08.020.

Al-Mahbashi, A.M., Elkady, T.Y. and Alrefeai, T.O. (2015), "Soil water characteristic curve and improvement in lime treated expansive soil", *Geomech. Eng.*, **8**(5), 687-696. https://doi.org/10.12989/gae.2015.8.5.687.

Baille, W., Tripathy, S. and Schanz, T. (2014), "Effective stress in clays of various mineralogy", *Vadose Zone J.*, **13**(5), 1-10. https://doi.org/10.2136/vzj2013.06.0112.

Birle, E., Heyer, D. and Vogt, N. (2008), "Influence of the initial water content and dry density on the soil-water retention curve and the shrinkage behavior of a compacted clay", *Acta Geotech.*, **3**(3), 191-200. https://doi.org/10.1007/s11440-008-0059-y.

Cai, G.Q., Zhou, A.N., Liu, Y., Xu, R.Z. and Zhao, C.G (2020), "Soil water retention behavior and microstructure evolution of lateritic soil in the suction range of 0-286.7 MPa", *Acta Geotech.*, **15**, 3327-3341. https://doi.org/10.1007/s11440-020-01011-w.

Chen, H.H., Li, L., Li, J.P. and Sun, D.A. (2022), "A generic analytical elastic solution for excavation responses of an arbitrarily-shaped deep opening under biaxial in-situ stresses", *J. Geotech. Geoenviron*., **22**(4), 04022023. https://doi.org/10.1061/(ASCE)GM.1943-5622.0002335.

Fredlund, D.G. and Rahardjo, H. (1993), *Soil Mechanics for Unsaturated Soils*, John Wiley & Sons, New York.

Fredlund, D.G. and Xing, A. (1994), "Equation for the soil-water characteristic curve", *Can. Geotech. J.*, **31**(4), 521-532. https://doi.org/10.1139/t94-061.

Gao, Y. and Sun, D.A. (2017), "Soil-water retention behavior of compacted soil with different densities over a wide suction range and its prediction", *Comput. Geotech.*, **91**, 17-26. https://doi.org/10.1016/j.compgeo.2017.06.016.

Gao, Y., Li, Z., Sun, D.A. and Yu, H.H. (2021), "A simple method for predicting the hydraulic properties of unsaturated soils with different void ratios", *Soil Till. Res.*, **209**, 104913. https://doi.org/10.1016/j.still.2020.104913.

Gao, Y., Sun, D.A., Zhou, A.N. and Li, J. (2018), "Effect of stress state on soil-water retention and its application on the strength prediction", *Geotech. Lett.*, **8**(4), 324-329. https://doi.org/10.1680/jgele.18.00159.

Greenspan, L. (1977), "Humidity fixed points of binary saturated aqueous solutions", *J. Res. Nat. Bureau Standard.*, **81**, 89-96. https://doi.org/ 10.6028/jres.081A.011.

Ito, M. and Azam, S. (2013), "Engineering properties of a vertisolic expansive soil deposit", *Eng. Geol.*, **152**(1), 10-16. https://doi.org/10.1016/j.enggeo.2012.10.004.

Konrad, J.M. and Lebeau, M. (2015), "Capillary-based effective stress formulation for predicting shear strength of unsaturated soils", *Can. Geotech. J.*, **52**(12), 2067-2076. https://doi.org/10.1139/cgj-2014-0300.

Lu, N. and Khorshidi, M. (2015), "Mechanism for soil-water retention and hysteresis at high suction range", *J. Geotech. Geoenviron*., **141**(8), 04015032. https://doi.org/10.1061/(ASCE)GT.1943-5606.0001325.

Miller, C.J., Yesiller, N., Yaldo, K. and Merayyan, S. (2002), "Impact of soil type and compaction conditions on soil water characteristic", *J. Geotech. Geoenviron.*, **128**(9), 733-742. https://doi.org/10.1061/(ASCE)1090-0241(2002)128:9(733).

Niu, G., Shao, L.T., Sun, D.A. and Guo, X.X. (2020), "A simplified directly determination of soil-water retention curve from pore size distribution", *Geomech. Eng.*, **20**(5), 411-420. https://doi.org/10.12989/gae.2020.20.5.411.

Péron, H., Hueckel, T. and Laloui, L. (2007), "An improved volume measurement for determining soil water retention curves", *Geotech. Test. J.*, **30**(1), 1-8. https://doi.org/10.1520/GTJ10016.

Rasool, A.M. and Kuwano, J. (2020), "Effect of constant loading on unsaturated soil under water infiltration conditions", *Geomech. Eng*., **20**(3), 221-232. https://doi.org/10.12989/gae.2020.20.3.221.

Romero, E., Gens, A. and Lloret, A. (1999), "Water permeability, water retention and microstructure of unsaturated compacted Boom clay", *Eng. Geol.*, **54**(1-2), 117-127. https://doi.org/10.1016/S0013-7952(99)00067-8.

Salager, S., Alessio, M., Ferrari, A. and Laloui, L. (2013), "Investigation into water retention behavior of deformable soils", *Can. Geotech. J.*, **50**(2), 200-208. https://doi.org/10.1139/cgj-2011-0409.

Sun, D.A., Gao, Y., Zhou, A.N. and Sheng, D.C. (2016), "Soil-water retention curves and microstructures of undisturbed and compacted Guilin lateritic clay", *Bull. Eng. Geol. Environ.*, **75**(2), 781-791. https://doi.org/10.1007/s10064-015.

Sun, D.A., Sheng, D.C. and Xu, Y.F. (2007), "Collapse behavior of unsaturated compacted clays with different initial densities", *Can. Geotech. J.*, **44**(6), 673-686. https://doi.org/10.1139/t07-023.

Sun, W.J. and Cui, Y.J. (2020), "Determining the soil-water retention curve using mercury intrusion porosimetry test in consideration of soil volume change", *J. Rock Mech Geotech*., **12**(5), 79-85. https://doi.org/10.1016/j.jrmge.2019.12.022.

Tan, Y.Z., Xu, X., Ming, H.J. and Sun, D.A. (2022), "Analysis of double-layered buffer in high-level waste repository", *Ann. Nucl. Energy*, **165**, 108660. https://doi.org/10.1016/j.anucene.2021.108660.

Tripathy, S., Tadza, M.Y.M. and Thomas, H.R. (2014), "Soil-water characteristic curves of clays", *Can. Geotech. J.*, **51**(8), 869-883. https://doi.org/10.1139/cgj-2013-0089.

Vanapalli, S.K., Pufahl, D.E. and Fredlund, D.G. (1999) "The effect of soil structure and stress history on the soil-water characteristics of a compacted till", *Geotechnique*, **49**(2), 143-159. https://doi.org/10.1680/geot.1999.49.2.143.

Wang, L., Sun, D.A., Yao, Y.P., Wu, L.Z. and Xu, Y.F. (2020). "Kinematic limit analysis of three-dimensional unsaturated soil slopes reinforced with a row of piles", *Comput. Geotech.*, **120**, 103428. https://doi.org/10.1016/j.compgeo.2019.103428.

Wang, L., Zhou, A.N., Xu, Y.F. and Xia, X.H. (2022), "Consolidation of partially saturated ground improved by impervious column inclusion: Governing equations and semi-analytical solutions", *J. Rock Mech Geotech.*, **14**(3), 837-850. https://doi.org/10.1016/j.jrmge.2021.09.017.

Wu, S.S., Zhou, A.N., Shen, S.L. and Kodikara, J. (2020), "Influence of different strain rates on hydro-mechanical behaviour of reconstituted unsaturated soil", *Acta Geotech.*, **15**, 3415-3431. https://doi.org/10.1007/s11440-020-01026-3.

Yang, H., Rahardjo, H., Leong, E.C. and Fredlund, D.G. (2004), "Factors affecting drying and wetting soil-water characteristic curves of sandy soils", *Can. Geotech. J.*, **41**(5), 908-920. https://doi.org/10.1139/t04-042.

Zhang, J.R., Niu, G., Li, X.C. and Sun, D.A. (2020), "Hydro-mechanical behavior of expansive soils with different dry densities over a wide suction range", *Acta Geotech.*, **15**(1), 265-278. https://doi.org/10.1007/s11440-019-00874-y.

Zhou, A.N., Sheng, D.C. and Li, J. (2014), "Modelling water retention and volume change behaviors of unsaturated soils in non-isothermal conditions", *Comput. Geotech.*, **55**(1), 1-13. https://doi.org/10.1016/j.compgeo.2013.07.011.

Zhou, B.C. and Lu, N. (2021), "Correlation between Atterberg limits and soil adsorptive water", *J. Geotech. Geoenviron.*, **147**(2), 04020162. https://doi.org/10.1061/(ASCE)GT.1943-5606.0002463.

Zhou, B.C., Zhao, X.X., Ma, Q.G. and Lang, M.T. (2020), "Soil-water retention term of 9 kinds of soils under high suctions", *Chin. J. Geotech. Eng.*, **43**(2), 236-244.

Zhu, Z.C., Sun, D.A., Zhou, A.N. and Qiu, Z.H. (2016), "Calibration of two filter papers at different temperatures and its application to GMZ bentonite", *Environ. Earth Sci.*, **75**(6), 509. https://doi.org/10.1007/s12665-015-5117-9.

CC